Time-Resolved Detection of Sensory Rhodopsin II-Transducer Interaction

Keiichi Inoue,* Jun Sasaki,† Masayo Morisaki,‡ Fumio Tokunaga,‡ and Masahide Terazima*
*Department of Chemistry, Graduate School of Science, Kyoto University, Kyoto, 606-8502, Japan; †Center for Membrane Biology, Department of Biochemistry and Molecular Biology, University of Texas Health Science Center, Houston, Texas 77030-1503 USA; and ‡Department of Earth and Space Science, Graduate School of Science, Osaka University, Osaka, 560-0055 Japan

ABSTRACT The dynamics of protein conformational change of *Natronobacterium pharaonis* sensory rhodopsin II (NpSRII) and of NpSRII fused to cognate transducer (NpHtrII) truncated at 159 amino acid sequence from the N-terminus (NpSRII-ΔNpHtrII) are investigated in solution phase at room temperature by the laser flash photolysis and the transient grating methods in real time. The diffusion coefficients of both species indicate that the NpSRII-ΔNpHtrII exists in the dimeric form in 0.6% dodecyl-β-maltopyranoside (DM) solution. Rate constants of the reaction processes in the photocycles determined by the transient absorption and grating methods agree quite well. Significant differences were found in the volume change and the molecular energy between NpSRII and NpSRII-ΔNpHtrII samples. The enthalpy of the second intermediate (L) of NpSRII-ΔNpHtrII is more stabilized compared with that of NpSRII. This stabilization indicates the influence of the transducer to the NpSRII structure in the early intermediate species by the complex formation. Relatively large molecular volume expansion and contraction were observed in the last two steps for NpSRII. Additional volume expansion and contraction were induced by the presence of ΔNpHtrII. This volume change, which should reflect the conformational change induced by the transducer protein, suggested that this is the signal transduction process of the NpSRII-ΔNpHtrII.

INTRODUCTION

Sensory rhodopsin II (SRII) is a retinal-containing protein found first in the membrane of an extremely halophilic archaeon, *Halobacterium salinarum*, along with the closely related microbial rhodopsins (Mukohata, 1994; Spudich et al., 2000), sensory rhodopsin I (SRI) (Bogomolni and Spudich, 1982), bacteriorhodopsin, and halorhodopsin (Mukohata, 1994). Unlike the latter two, which function as light-driven proton and chloride pumps, respectively, SRI and SRII have been identified as photoreceptors for the positive phototaxis toward orange-red light (Spudich and Bogomolni, 1984) and for the negative phototaxis response to evade blue-green light (Takahashi et al., 1985; Spudich et al., 1986), respectively. The taxis signal regulation by the photoreceptors is enabled by association with chemotaxis transducer-like proteins (HtrI) (Yao and Spudich, 1992) and HtrII (Seidel et al., 1995; Zhang et al., 1996), which are in complex with SRI and SRII, respectively.

These microbial rhodopsins consist of a single peptide made up of seven transmembrane α-helices (A–G) and a chromophore retinal covalently bound through a protonated Schiff base linkage to a lysine residue at the seventh helix. Photoexcitation of the chromophore retinal elicits all-*trans* to 13-*cis* isomerization, which initiates structural changes of the protein moiety. These changes, which affect the electric environment of the chromophore, have been spectroscopically identified as quasi-stable intermediate states, named K, L, M, N, and O, in the order of their appearance (Imamoto et al., 1991; Chizhov et al., 1998). At the end of the reaction sequence, the molecule restores the initial state, and thereby the cyclic reaction is called a photocycle. In SRI and SRII, it is presumed that the conformational changes are transmitted to the associated HtrI and HtrII, respectively, through the interacting transmembrane domain of the transducer (Zhang et al., 1999).

SRII and HtrII were also found in another archaeon, *Natronobacterium pharaonis* (denoted as NpSRII and NpHtrII, respectively) (Hirayama et al., 1992; Seidel et al., 1995). They were shown to be functional for eliciting negative phototaxis for blue-green light when they were expressed in *H. salinarum* (Lüttenberg et al., 1998), showing that the complex undergoes identical conformational changes as does the SRII-HtrII complex of *H. salinarum* (HsSRII-HsHtrII) and are capable of associating with the downstream signal-transduction-cascade components of *H. salinarum*. Since NpSRII is very stable at various salt concentrations and can be produced in abundance in an *Escherichia coli* expression system (Simono et al., 1997), significant advances in the photochemical and structural analyses have been made by the use of NpSRII. Indeed, x-ray crystallographic structures of the free receptor (Luecke et al., 2001; Royant et al., 2001) and of the receptor complexed with a truncated NpHtrII have been obtained by the use of NpSRII (Gordelly et al., 2002).

NpHtrII is a homolog of methyl-accepting-chemoreceptor proteins (MCPs) (Falke and Hazelbauer, 2001; Stock et al., 2002; Parkinson, 2003), which form stable homodimers consisting of elongated helical bundle oriented normal to the membrane. Methyl-accepting-chemoreceptor proteins are anchored to the membrane with two transmembrane helices (TM1 and TM2) forming a four helical bundle in the dimer,

Submitted March 24, 2004, and accepted for publication July 7, 2004.

Address reprint requests to Masahide Terazima, Tel.: 81-75-753-4026; Fax: 81-75-753-4000; E-mail: mterazima@kuchem.kyoto-u.ac.jp.

0006-3495/04/10/2587/11 $2.00

doi: 10.1529/biophysj.104.043521

with a periplamic ligand-binding domain connected between TM1 and TM2 and the cytoplasmic domain after TM2, which is a helical hairpin forming four helical bundle in the homodimer. One helix in each subunit extends the entire length of the structure, connecting the ligand-binding site at the membrane-distal end of the periplasmic domain with the kinase-interaction region at the opposite end of the receptor.

NpHtrII is missing the periplasmic ligand-binding site but instead associates through TM1 and TM2 with F and G helices of NpSRII (Gordelly et al., 2002). However, because the crystal structure resolves only the two transmembrane domains (N-terminal 22–80 out of 543 amino acid residues), the possibility that the unresolved cytoplasmic domain also participates in the association cannot be excluded. In fact, isothermal titration calorimetry measurement revealed that an N-terminal sequence of 114 amino acids of NpSRII was the minimum required for tight binding ($K_d \sim 240$ nM) (Hippler-Mreyen et al., 2003), indicating ~30 residues in the cytoplasmic domain also associate with NpSRII in addition to the transmembrane domain.

Binding of the transducer to the photoreceptor protein was also demonstrated by the inhibition of proton uptake from the cytoplasmic channel of the photoreceptor (Bogomolni et al., 1994; Schmies et al., 2000; Hippler-Mreyen et al., 2003) and by alteration of the kinetics of the photocycle intermediate decay rates (Spudich and Spudich, 1993; Sasaki and Spudich, 1998; Sudo et al., 2001, 2002). The particular intermediates whose decay rates were affected in the presence of the transducer molecules have been identified as the signaling state, in which conformational changes of the photoreceptors are transmitted to the transducers. However, in view of that, this effect is subtle in the case of NpSRII-NpHtrII interaction, and considering that changes in the rate constants do not reflect energetic stability of the intermediate state but activation energy for crossing over barriers during the conversion, the alteration in the rate constants does not necessarily provide criterion for identifying signaling state intermediates.

To reveal the signal transduction process in time, it is indispensable to monitor the protein dynamics not only of the kinetic effect but also of the conformational change, because the signal transfer occurs through the conformational change.

Recently, one of us showed that the time development of protein conformational changes can be monitored through the volume changes, because the partial molar volume is sensitive to the protein conformation (Sakakura et al., 2001; Nishioku et al., 2001; Takeshita et al., 2002). For monitoring time-dependent volume change, the pulsed-laser induced time-resolved transient grating (TG) technique (Terazima and Hirota, 1993) has been used. In this method, a sinusoidal modulation of the light intensity is produced by the interference of two light waves. Photoexcitation of the sample by this light creates a sinusoidal modulation in the refractive index (δn) due to the temperature change as well as the volume change. These changes are detected as the diffraction of another probe beam. Therefore, the protein conformational change can be monitored as the time development of the TG signal. We applied this technique to monitor conformational changes of a truncated NpHtrII as well as those of free NpSRII in time domain. Here we used a truncated NpHtrII that ends at the 159th amino acid from the N-terminus (ΔNpHtrII), which ensures tight binding to the receptor and yet contains ~70 amino acid sequence of the cytoplasmic domain that contains a region for coiled-coil formation. We further designed the molecules so that NpSRII and ΔNpHtrII are fused at the C-terminus and the N-terminus, respectively, through a nine amino acid linker sequence, which was already proven not to interfere with the function in vivo (Jung et al., 2001; Chen and Spudich, 2002).

Energies and volume changes in the early step of NpSRII photocycle have been reported using the photoacoustic (PA) method previously (Losi et al., 1999, 2001a), and also this technique was applied to other photoreaction systems including rhodopsins (Braslavsky and Heibel, 1992; Losi et al., 2001b; Losi and Braslavsky, 2003; Zhang and Mauzerall, 1996). The PA method is complementary to the TG method. There are significant advantages, however, in the time-resolved TG method over the conventional PA method. First, the volume change and the enthalpy change of the protein can be determined in time domain without temperature variation or solvent variation method. This advantage is useful because the volume changes, and the energy changes of proteins during the reactions could depend on the temperature sensitively (Sakakura et al., 2001; Takeshita et al., 2002). Second, the time window of the TG method is quite wide compared with the PA method. We can trace the dynamics from 20 ns to several seconds continuously to cover all the reaction steps of NpSRII. Third, the molecular diffusion can be detected, which provides a valuable information on the states of proteins. On the other hand, there is a disadvantage; the sources of the signal, the refractive index change, do not come only from the volume change and enthalpy change but also from corresponding absorption spectrum change (population grating), which sometimes disturbs a measurement of the conformational change and the enthalpy change. However, we can overcome this problem by using several techniques including the q^2-dependence measurement or the comparison method between the results of NpSRII and the fusion protein as we used in this research. Using these advantages, we studied the protein-protein interaction of the NpSRII-ΔNpHtrII complex from a viewpoint of volume changes for the first time.

EXPERIMENTAL PROCEDURES

The *H. salinarum* strain that produces free NpSRII carries an expression plasmid vector (pJS005), which contains the *NpsopII* gene followed by HSESHHHHHH at the C-terminus under the control of the *bop* promoter as described previously (Krebs et al., 1995; Kunji et al., 2001). The *H. salinarum* strain produces a fusion protein of NpSRII and a truncated

NpSRII (ΔNpHtrII) at the 159th residue are connected through a nine amino acid linker (ASASNGASA) between the C-terminus of NpSRII and the N-terminus of the truncated HtrII. The plasmid vector containing the gene of fusion protein with the full length of NpHtrII (pJS009) was constructed previously (Jung et al., 2001). The truncated fusion protein gene was made by polymerase chain reaction (PCR) with pJS009 as a template and with the forward primer TCACCGGACGTCCCATGGTG and reverse primer AATATGCATTAGTTCCGTGTTGATCTCCTC. The forward primer contains a forward sequence of initiation codon followed by the beginning of the *NpsopII* gene, and the reverse primer contains a reverse sequence of the 159th residue followed by *Nsi*I restriction site. The polymerase chain reaction fragment was treated with restriction enzymes *Nco*I and *Nsi*I and ligated to the same expression vector as pJS009. This construct (named pNT19) thus contains the gene for the fusion protein of NpSRII linked at the C-teminus to the nine amino acid linker, which is then fused to the N-terminus of NpHtrII truncated at the 159th residue followed by HSESHHHHHH. A halobacterial strain devoid of any one of rhodopsin genes and *htrI*, *htrII* genes (Pho-81) was transformed with pNT19 as described elsewhere (Krebs et al., 1993).

The transformants of *H. salinarum* were cultured in 8 l complex medium containing 1 μg/ml mevinolin (Krebs et al., 1993) at 37°C with vigorous aeration from an air pump and under illumination from a fluorescent light for ~10 days. The membrane fraction of the cells was harvested in a conventional method (Krebs et al., 1993). It was then solubilized in 1% dodecyl-β-maltopyranoside (DM) (Wako, Osaka, Japan), 50 mM MES (pH 6.0), 4 M NaCl, and 5 mM imidazole. The solute was incubated with Ni-NTA resin and shaken gently for >4 h so that his-tagged protein was bound to the resin. The resin was loaded on a column and washed with ~20 volume of 0.06% DM in the same buffer and eluted in 0.06% DM containing 50 mM sodium acetate (pH 4.0), 4 M NaCl, and 5 mM imidazole. The pH was then adjusted to 7.0 by adding 1.0 M Tris-HCl buffer. The protein was reconcentrated with CENTRICON 10,000 Da molecular mass (Millipore, Bedford, MA). The sample used in this measurement contains ~200 μM in 0.06% DM, 4 M NaCl, 50 mM sodium acetate, 5 mM imidazole, and 115 mM Tris-HCl.

The TG setup was similar to that described previously (Terazima and Hirota, 1993; Hara et al., 1996; Nishioku et al., 2001). Briefly, the beam of a XeCl excimer laser-pumped dye laser (Lambda Physik Compex 102xc, Göttingen, Germany, Lumomics Hyper Dye 300; $\lambda = 465$ nm) was divided by a beam splitter and the beams crossed inside a quartz sample cell (optical pathlength = 2 mm). The laser power of the excitation was <1.0 μJ/pulse. The interference pattern (transient grating) created in the sample was probed by a diode laser (780 nm) as a Bragg diffracted signal (TG signal). The signal was detected by a photomultiplier tube (Hamamatsu R-1447, Hamamatsu, Japan) and recorded by a digital oscilloscope (Tektronix TDS-5052, Beaverton, OR). The grating wavenumber, q, was varied by changing the crossing angle of the excitation and probe beams.

For the transient absorption (TA) measurements, the same dye laser was used for the excitation, and the absorption change was probed at 543.5 nm. The change of the light intensity of the probe light was monitored with the photomultiplier tube, and the time profile was recorded by the digital oscilloscope.

We were extremely careful for the data acquisition condition. The repetition rate of the excitation laser was less than 0.23 Hz to prevent the multiexcitation of the intermediate species before recovering to the original NpSRII. The excitation beam was slightly focused to the sample with a 1-mm diameter. The light irradiated volume was $\sim 1.5 \times 10^{-3}$ ml. Furthermore, we used a laser power for the excitation as low as possible, typically 0.6 μJ/pulse, for quantitative ΔH and ΔV measurements. The TA and TG signals were averaged ~100–200 shots data, and experiments were repeated several times for examining the reproducibility.

Experiments were performed at 21°C. Bromocresol purple (BCP) in aqueous solution was used as a reference to determine q^2 from the decay rate of the thermal grating signal and known thermal diffusivity of water. Since the lifetimes of the excited states of bromocresol purple are less than 1 ns, and the radiative transitions as well as photochemical reaction are negligible, all of the absorbed photon energy should be released within the pulse width of our excitation laser to create only the thermal grating signal. For quantitative measurement of the signal intensity, we used cytochrome c in the same buffer solution as a calorimetric reference sample. The absorbance of cytochrome c was adjusted to the same value as that of the sample at the excitation wavelength.

PRINCIPLES

Under weak diffraction conditions, the TG signal intensity (I_{TG}) is proportional to the square of the variations in the refractive index (δn) and in the absorbance (δk). We can neglect the δk term by selecting a probe wavelength at which the absorption change is sufficiently small. The refractive index change consists of the following three components: temperature rise due to the released thermal energy (δn_{th}, thermal grating), the molecular refractive index difference between the reactant and products due to the change of the absorption spectrum (δn_{pop}, population grating), and the density change caused by the reaction volume (δn_v, volume grating). We call the sum of δn_{pop} and δn_v the species grating (δn_{spe}) because the time profiles of δn_{pop} and δn_v are identical for most cases. The TG signal intensity (I_{TG}) is given by

$$I_{TG}(t) = \alpha\{\delta n_{th}(t) + \delta n_{pop}(t) + \delta n_v(t)\}^2, \qquad (1)$$

where α is a constant representing the sensitivity of the system.

The temporal evolution of $\delta n_{th}(t)$ reflects the time dependence of the thermal energy being released. Solving the thermal diffusion equation, one obtains (Terazima, 1998)

$$\delta n_{th}(t) = \left(\frac{dn}{dT}\right)\frac{W}{\rho C_P}[dQ(t)/dt \otimes \exp(-D_{th}q^2 t)], \qquad (2)$$

where $\otimes$ represents the convolution integral, $Q(t)$ is the thermal energy coming out from the photoexcited sensory rhodopsin, W is molecular weight of the solvent, dn/dT is the temperature dependence of the refractive index, ρ is the density of the solvent, C_p is the heat capacity at constant pressure, and D_{th} is the thermal diffusivity. The grating wavenumber q is given by $q = \pi\sin(\theta/2)/\lambda_{ex}$ (λ_{ex} is the wavelength of the excitation light). By analyzing the time profile of the thermal grating signal with Eq. 2, the thermal energy associated with each reaction process can be measured. The enthalpy of each species (ΔH) is defined by the enthalpy difference from that of the original species,

$$Q(t) = \Delta N(h\nu - \Phi\Delta H), \qquad (3)$$

where Φ is the quantum yield of the reaction, ΔN is the number of the reacting molecules in a unit volume, and $h\nu$ is the photon energy for the excitation. By a quantitative measurement of the thermal grating signal intensity, the enthalpy of each species can be calculated. The proportion-

ality constant α in Eq. 1 can be determined by comparison of the signal intensity with that of the calorimetric reference sample, which releases the absorbed photon's energy as thermal energy within our time resolution. The refractive index change after photoexcitation of a calorimetric reference sample (δn_{th}(reference)(t)) is given by

$$\delta n_{\mathrm{th}}(\mathrm{reference}) = \left\{\left(\frac{dn}{dT}\right)\frac{\Delta N h\nu W}{\rho C_{\mathrm{P}}}\right\}\exp(-D_{\mathrm{th}}q^2t) = \delta n^0_{\mathrm{th}}(\mathrm{reference})\exp(-D_{\mathrm{th}}q^2t). \quad (4)$$

By taking a ratio of amplitude of the thermal grating signal of sample (δn_{th}(sample))/δn^0_{th} (reference), ΔH can be calculated by

$$\frac{\delta n(\mathrm{sample})}{\delta n(\mathrm{reference})} = 1 - \frac{\Phi\Delta H}{h\nu}. \quad (5)$$

A difficulty we may encounter for measuring ΔH of an intermediate species is that the species grating signal interferes the thermal grating signal. We have to properly estimate the species grating contribution. In some cases, the species grating signal has been estimated by using the temperature dependence method (Nishioku et al., 2002). This method is based on a fact that δn_{th} is proportional to dn/dT, which is strongly dependent on temperature for aqueous solution. By the measurement at around 0°C, at which dn/dT almost vanishes, the species grating signal can be measured without the contribution of δn_{th}. However, using the temperature dependence method, we have to always assume that the other contribution does not depend on temperature, which is frequently not correct for protein reactions. Therefore, here, we use another method to determine δn_{th}.

The method is based on the fact that the time profile of the species grating signal is determined by the chemical reaction, whereas the thermal grating decays with a rate constant of $D_{\mathrm{th}}q^2$, which can be varied by changing the crossing angle of the excitation beams. Therefore, by analyzing the TG signal at various q^2, we can separate the δn_{th} term from the δn_{spe} term. Qualitatively, the thermal grating signal intensity that decays with a rate constant of $D_{\mathrm{th}}q^2$ reflects the thermal energy released until this time. By changing q^2 and hence $D_{\mathrm{th}}q^2$, the time window in which we can monitor the thermal energy can be changed; i.e., the enthalpy of intermediate species in various time range can be determined by gradual changing of $D_{\mathrm{th}}q^2$. Quantitatively, the thermal grating signal intensity with a rate constant of $D_{\mathrm{th}}q^2$ is given by

$$\delta n_{\mathrm{th}}(t) = \delta n_{\mathrm{th},1} + \frac{k_1}{k_1 - D_{\mathrm{th}}q^2}\delta n_{\mathrm{th},2} + \frac{k_1k_2}{k_2 - k_1}\left\{\frac{1}{k_1 - D_{\mathrm{th}}q^2} - \frac{1}{k_2 - D_{\mathrm{th}}q^2}\right\}\delta n_{\mathrm{th},3},$$

where $\delta n_{\mathrm{th,i}}$ and k_{i} are refractive index changes by heat released on production of intermediate species i and reaction rate of this species, respectively. Therefore, we can determine $\delta n_{\mathrm{th,i}}$ through the $D_{\mathrm{th}}q^2$ dependence of $\delta n_{\mathrm{th}}(t)$. Once we can separate the thermal grating terms, taking a ratio of $\delta n_{\mathrm{th,i}}/\delta n_{\mathrm{th}}$(reference) enables us to determine ΔHs of each intermediates from Eq. 5. By this way, ΔH at a constant temperature without disturbance of the species grating signal intensity can be obtained.

The refractive index change due to the volume grating is given by

$$\delta n_{\mathrm{v}} = V\frac{dn}{dV}\Delta V\Delta N, \quad (6)$$

where Vdn/dV is the refractive index change by the molecular volume change. By taking a ratio of $\delta n_{\mathrm{v}}/\delta n_{\mathrm{th}}$(reference) with the known solvent property (Vdn/dV), ΔV is determined.

The time dependence of the species grating is determined by the kinetics of the reaction and the molecular diffusion process. If we can neglect the reaction kinetics in the molecular diffusion time region, the time dependence is given by (Terazima and Hirota, 1993; Hara et al., 1996)

$$\delta n_{\mathrm{spe}}(t) = -\delta n_{\mathrm{r}}\exp(-D_{\mathrm{r}}q^2t) + \delta n_{\mathrm{p}}\exp(-D_{\mathrm{p}}q^2t), \quad (7)$$

where δn_{r} and δn_{p} represent refractive index changes by the reactant and product, respectively. D_{r} and D_{p} are the molecular diffusion coefficients of the reactant and product, respectively. The reaction kinetics can be separated from the diffusion process by measuring the transient grating dynamics at different q^2 because the diffusion process depends on q^2, whereas the reaction kinetics should not.

RESULTS

Kinetics of the reaction

The reaction kinetics of the photocycle for the free NpSRII have been studied under similar experimental conditions to ours (Chizhov et al., 1998). Effects of complexation of NpHtrII and ΔNpHtrII on the photocycle kinetics, for which NpSRII and NpHtrII were separately prepared and were combined to form complex, were shown to slow the decay of the M state so that it decays at the end of the photocycle together with the O state. Our preliminary time-resolved visible spectral measurement at ~1-ms time resolution showed that the fusion protein of NpSRII-ΔNpHtrII also showed similar effect on the photocycle (not shown), indicating that, in the fusion molecules, NpSRII and ΔNpHtrII interact with each other in the same way as the separated two molecules combined (Sudo et al., 2001).

Before showing the results of the TG measurements, the kinetics monitored by the transient absorption method is roughly described. We measured the time profile of the TA

signal of NpSRII and NpSRII-ΔpHtrII at 543.5 nm, where formation of red-shifted intermediates such as K and O contribute to the increase of the signal, whereas formation of blue-shifted intermediates such as L and M cause the decrease of the signal. The signal of NpSRII is shown in Fig. 1 *a*. The time profile in the monitoring time region (400 ns ~ 1 s) can be fitted well with a sum of six exponential functions:

$$I_{TA}(t) = a_1 \exp(-k_1 t) + a_2 \exp(-k_2 t) + a_3 \exp(-k_3 t) + a_4 \exp(-k_4 t) + a_5 \exp(-k_5 t) + a_6 \exp(-k_6 t). \quad (8)$$

The determined preexponential factors (a_1–a_6) and the rate constants (k_1–k_6) are listed in Table 1. Wegener et al. reported eight phases in the photocycles of NpSRII and NpSRII-ΔpHtrII. The rate constants are in a range of $0.91 \times 10^6\ s^{-1} \sim 0.71\ s^{-1}$ and $1.0 \times 10^6\ s^{-1} \sim 1.1 s^{-1}$ for NpSRII and NpSRII-ΔpHtrII, respectively (Wegener et al., 2000). Although some of the rate constants are not exactly the same as those reported previously, the time ranges of the dynamics are roughly similar. The difference may come from the different experimental conditions.

Attribution of the kinetics obtained here to each of the conversion between the intermediates especially in the latter half of the photocycle is not as simple. In this study, we do not attempt to identify these kinetics. However, for convenience, we tentatively use the following assignment of these kinetics for describing the TG results.

$$\text{NpSRII} \xrightarrow{k_1} \text{K} \xrightarrow{k_2} \text{L} \xrightarrow{k_3} \text{M} \xrightarrow{k_4} \text{M}' \xrightarrow{k_5} \text{M}'' \xrightarrow{k_6} \text{O} \rightarrow \text{NpSRII}.$$

(Scheme 1)

Fig. 1 *b* shows the TA signal of NpSRII-ΔpHtrII. The time profile is very similar to that of NpSRII. The rate constants and the preexponential factors are listed in Table 1. We may notice that the amplitudes and rate constants are relatively similar for both samples.

TG signal

Fig. 2 *a* shows the TG signal after the photoexcitation of NpSRII at $q^2 = 6.5 \times 10^{10}\ m^{-2}$. The signal rises first with a rate of our system response (~50 ns) and, then, rises gradually until ~100 μs. At this q^2, the signal slightly decays, turns to rise again, and finally decays to the baseline. We found that the time profile in this wide time range (100 ns–100 ms) can be reproduced well by a sum of seven exponential functions. Most of the rate constants except two of them are very similar to those determined by the TA method in the previous section (k_1, k_2, k_3, k_4, and k_5 in Eq. 8). Furthermore, these rate constants do not depend on q^2. Hence, these are attributed to the intrinsic reaction kinetics.

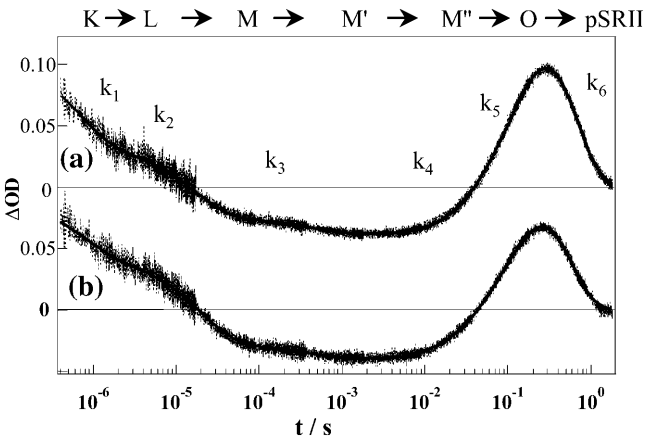

FIGURE 1 The kinetic traces of the transient absorption signals (*dotted lines*) and the best fitted curves (*solid lines*) by Eq. 8 of (*a*) NpSRII and (*b*) NpSRII-ΔNpHtrII in 0.06% DM, 4 M NaCl, 50 mM sodium acetate, 5 mM imidazole, and 115 mM Tris-HCl solution. The sample solutions are photoexcited at 465 nm and probed at 543.5 nm. The rough timescales for each exponential terms and the assignment based on Scheme 1 are described in the figure.

There are two rate constants that are very much different from those from the TA signal. The rate constant of the faster one agrees well with the decay rate constant of the thermal grating signal from the calorimetric standard sample, which is given by $D_{th}q^2$. Indeed, measuring the TG signal at different q^2, we found that the decay rate is proportional to q^2. Hence, we can definitively assign this contribution to the thermal grating signal. The other q-dependent decay rate constant corresponds to the final step of the decay. According to the theoretical expression described in Principles, this decay rate represents the molecular diffusion process and the intrinsic reaction rate. Hence, the TG signal in the whole time range should be analyzed by

$$I_{TG}(t) = \alpha\{\delta n_{th} \exp(-D_{th}q^2 t) + \delta n_1 \exp(-k_1' t) + \delta n_2 \times \exp(-k_2' t) + \delta n_3 \exp(-k_3' t) + \delta n_4 \exp(-k_4' t) + \delta n_5 \exp(-k_5' t) + \delta n_6 \exp(-k_6' t)\}^2, \quad (9)$$

where the sign of the preexponential factors of δn_1, δn_2, δn_3, and δn_4 are positive and the others (δn_{th}, δn_5, and δn_6) are negative. Here, the rate constant of k_6' can be written as $D_{pSR}q^2 + k_6$, where D_{pSR} is the diffusion coefficient of NpSRII. Indeed, plotting k_6' against q^2, we found a linear relationship with a positive intercept at $q^2 = 0$ (Fig. 3). From the linear fitting using $k_6 = 4.2\ s^{-1}$, D_{pSR} is determined from the slope to be $(3.4 \pm 0.3) \times 10^{-11}\ m^2/s$.

The TG signal of NpSRII-ΔNpHtrII is shown in Fig. 2 *b*. The signal is very similar to that of NpSRII and can be expressed by Eq. 9. The preexponential factors and the rate constants are listed in Table 1. Comparing these parameters with those of NpSRII, we note several differences. First, although most of the preexponential factors are similar for

TABLE 1 Rate constants (upper) and the preexponential factors (lower) for the best fitting of the transient absorption (TA) and transient grating (TG) signals for NpSRII and NpSRII-ΔNpHtrII

Method	Sample	$k_1/10^6$ s^{-1}	$k_2/10^5$ s^{-1}	$k_3/10^3$ s^{-1}	$k_4/10$ s^{-1}	k_5/s^{-1}	k_6/s^{-1}
TA	NpSRII	1.5 ± 0.1	6.7 ± 0.1	2.4 ± 0.1	8.3 ± 0.5	7.7 ± 0.1	4.2 ± 0.1
	NpSRII-ΔNpHtrII	1.6 ± 0.1	3.9 ± 0.1	2.6 ± 0.7	8.3 ± 0.2	10 ± 0.2	3.7 ± 0.1
TG	NpSRII	1.4 ± 0.2	5.6 ± 0.4	2.7 ± 0.5	12 ± 2	7.7 ± 0.1	4.6 ± 0.1
	NpSRII-ΔNpHtrII	1.4 ± 0.3	5.0 ± 0.8	2.9 ± 0.5	14 ± 1	11 ± 0.2	4.0 ± 0.1
Method	Sample	a_1, δn_1	a_2, δn_2	a_3, δn_3	a_4, δn_4	a_5, δn_5	a_6, δn_6
TA	NpSRII	0.87 ± 0.1	1.0	0.20 ± 0.1	0.17 ± 0.1	−5.6 ± 0.1	4.9 ± 0.1
	NpSRII-ΔNpHtrII	0.67 ± 0.1	1.0	0.15 ± 0.1	0.11 ± 0.1	−5.5 ± 0.2	4.9 ± 0.2
TG	NpSRII	1.1 ± 0.1	1.3 ± 0.2	0.25 ± 0.1	0.24 ± 0.1	−1.3 ± 0.2	−1.3 ± 0.2
	NpSRII-ΔNpHtrII	0.94 ± 0.1	1.9 ± 0.2	0.23 ± 0.1	0.22 ± 0.1	−0.59 ± 0.1	−2.2 ± 0.3

The preexponential factors of the TA signals (a_i: $i = 1$–6) are normalized by a_2. The preexponential factors of the TG signals (δn_i: $i = 1$–6) are normalized by δn_{th}(reference) measured under the same experimental condition.

both samples, the preexponential factors of δn_5 and δn_6 are different. We will discuss this point later. Secondly, we found that the decay rate constant of the final step (k'_6) is slower for NpSRII-ΔNpHtrII than that for NpSRII. As mentioned above, this decay rate should represent the molecular diffusion of NpSRII-NpHtrII and the intrinsic reaction rate. From the plot of k'_6 against q^2 (Fig. 3), the diffusion coefficient of NpSRII-ΔNpHtrII ($D_{\text{pSR-H}}$) is determined to be $(1.8 \pm 0.2) \times 10^{-11}$ m^2/s. Hence the slower rate of the final step is due to the smaller D compared with D_{pSR} ($D_{\text{pSR-H}}/D_{\text{pSR}} = 0.53$).

Enthalpy changes

The origin of the thermal grating signal is the thermal energy due to the nonradiative transition and the enthalpy changes accompanying the photoreaction of NpSRII. Therefore, if we can measure the time profile of the thermal grating signal in time domain, we can determine the enthalpies of the intermediates step by step from the intensities of the signals. A difficulty we encounter for the quantitative measurement of the thermal grating signal comes from interference by the species grating signal. We separate the thermal grating and the species grating contributions by the q-dependence method described in Principles. For the quantitative measurement of the signal intensity, we were careful with the excitation laser power. When the excitation laser power was too high, multiphoton excitation takes place; i.e., one of the intermediate species absorbs another photon, which should be released as heat eventually. As the consequence, the thermal grating signal intensity increases. Comparing the thermal grating intensity with that of the species grating with increasing excitation laser power, this effect became noticeable above ~1.0 μJ/pulse of the excitation. Thus we used sufficiently weak power for the excitation (<0.6 μJ/pulse).

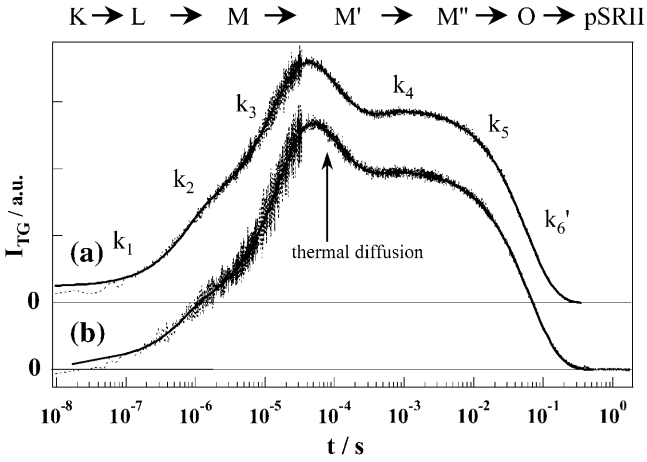

FIGURE 2 The TG signals of (*dotted lines*) and the best fitted curves (*solid lines*) by Eq. 9 of (*a*) NpSRII and (*b*) NpSRII-ΔNpHtrII after photoexcitation at 465 nm and probed at 780 nm. The rough timescales for each exponential terms and the assignment based on Scheme 1 are described in the figure.

Using this method, we evaluate the pure species grating signal and subtract it from the observed signal to obtain the pure thermal grating signals. The temporal profiles of the pure thermal grating signals at $q^2 = 6.5 \times 10^{10}$ m^{-2} of NpSRII and NpSRII-ΔNpHtrII are shown in Fig. 4. We notice an interesting difference between these signals. Although the signal rises with the lifetime of 18 μs and decays to the baseline with $D_{th}q^2$ for the NpSRII sample (*solid line*), it shows almost monotonically decays by the thermal diffusion process for the NpSRII-ΔNpHtrII sample (*dotted line*). The rise of the thermal grating signal indicates that the thermal energy is released with this rate, which reflects the energetic relaxation. We determine $\Phi\Delta H$ by the method described in Experimental Methods. Assuming Φ of M intermediate formation (Φ_M) for NpSRII ($\Phi_M = 0.46$) (Losi et al., 1999) and for NpSRII-ΔNpHtrII ($\Phi_M = 0.4$) (Losi et al., 2001a), and also assuming that the quantum yield of L → M and the following thermal steps is unity, the ΔH values of the L and M species are determined to be 169 ± 5 kJ/mol and 60 ± 6 kJ/mol for NpSRII, respectively, whereas they are 81 ± 2 kJ/mol and 81 ± 7 kJ/mol for NpSRII-ΔNpHtrII (Fig. 5). Previously, Nishioku et al. have reported

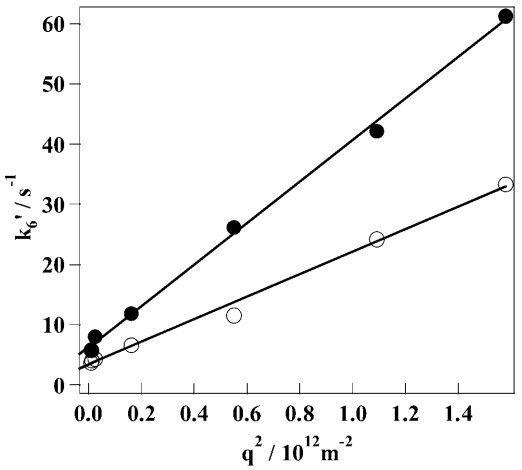

FIGURE 3 Plots of the rate constant of k'_6 against q^2 of NpSRII (●) and NpSRII-ΔNpHtrII (○). The solid lines are the best fitted lines by a relation of $k'_6 = Dq^2 + k_6$. The slope of the fitted line corresponds to the diffusion coefficient, and the intercept at $q^2 = 0$ indicates the intrinsic rate constant of the reaction.

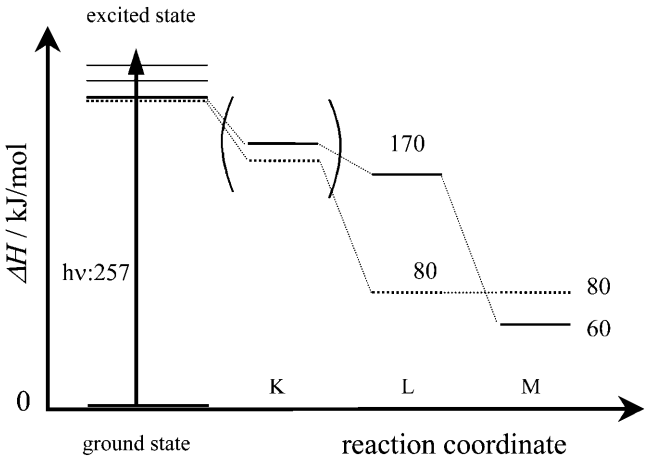

FIGURE 5 Schematic energy levels of early intermediates of NpSRII (*solid lines*) and NpSRII-ΔNpHtrII (*broken lines*). The energy levels of the K intermediate cannot be determined in this experiment. The enthalpies of these levels are described in the figure.

that the energy of the octopus rhodopsin is stabilized significantly from the Lumi (L of NpSRII) intermediate (122 kJ/mol) to the Meso (M of NpSRII) (38 kJ/mol) (Nishioku et al., 2001). The observed large energy stabilization from L to M intermediates in the NpSRII case is similar to that of octopus rhodopsin.

Using the PA method, Losi et al. reported the enthalpy of the K intermediate of NpSRII (NpSRII-His in their description) to be 134 kJ/mol (Losi et al., 1999). Our ΔH value is higher than this value. The difference may come from two origins. First, as Losi et al. reported, the energies of early intermediates (K and L) depend on contents of solvent (Losi et al., 2001a), especially sodium chloride. Our sample contains a 20–30 times higher concentration of NaCl than theirs. This different concentration could change the energies of the intermediate. Second, they used the temperature dependence method for the separation of ΔH and ΔV. However, it is possible that the ΔH and ΔV values depend on temperature as we have shown before for other proteins (Takeshita et al., 2002; Sakakura et al., 2001). The accurate ΔH and ΔV should be measured at a constant temperature as we did in this work.

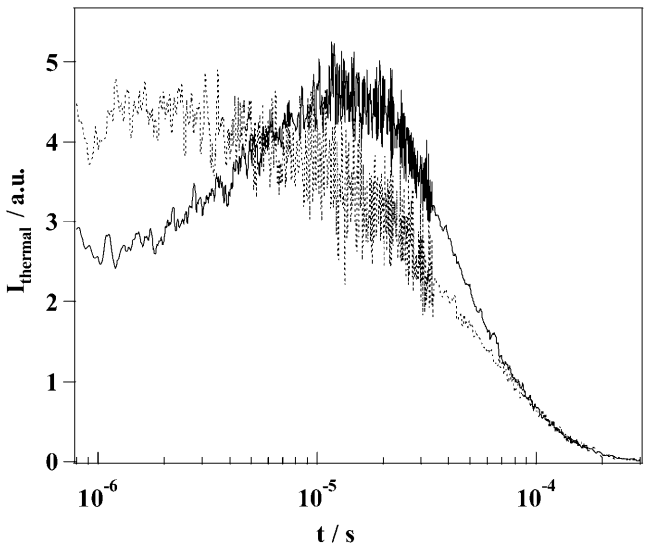

FIGURE 4 Pure thermal grating signals ($I_{thermal}$) of NpSRII (*solid line*) and NpSRII-ΔNpHtrII (*dotted line*) obtained by subtracting species grating signals from the observed signals.

Volume change

Most of the preexponential factors of the TG signals between NpSRII and NpSRII-ΔNpHtrII are similar to each other except δn_5 and δn_6. In this section, we consider the amplitude of the species grating signal, which consists of the population and volume grating contributions.

The refractive index change due to the change of the absorption spectrum (population grating term) can be calculated by the Lorenz-Lorentz relationship and the corresponding absorption spectrum. The absorption spectra of NpSRII including the intermediate species are almost identical to those of NpSRII-ΔNpHtrII. Indeed, the amplitudes of the transient absorption components observed in this study are similar (Table 1). The similarity of both absorption spectra lead us to expect that the amplitude of the population grating components between NpSRII and NpSRII-ΔNpHtrII should be similar each other, too. Therefore, the difference in the volume grating contributions can be estimated from the difference in the species grating amplitudes between NpSRII and NpSRII-ΔNpHtrII. Based on these considerations, the similar amplitudes for $\delta n_1 \sim \delta n_4$ between NpSRII and NpSRII-ΔNpHtrII suggest that the conformational changes

up to M intermediate are similar for NpSRII and NpSRII-ΔNpHtrII, that is, the conformational changes do not depend on the presence of ΔNpHtrII for these intermediates.

On the other hand, the species grating terms of δn_5 and δn_6 are different between NpSRII and NpSRII-ΔNpHtrII, indicating that the volume changes depend on the presence of ΔNpHtrII. However, it is difficult to determine the value of this volume change for each species because the absolute magnitude of the population grating contribution cannot be estimated. On the other hand, the difference in ΔV associated with O → NpSRII transition between NpSRII and NpSRII-ΔNpHtrII ($\Delta\Delta V_{\text{O-NpSRII}}$) can be estimated from δn_6 as follows. The preexponential factor δn_6 is related with the refractive index change associated with O → NpSRII transition ($\delta n_{\text{O-NpSRII}}$). Hence, the population grating contribution can be cancelled out by taking the difference between NpSRII and NpSRII-ΔNpHtrII ($\delta n_{\text{O-NpSRII}}$ (NpSRII-ΔNpHtrII) − $\delta n_{\text{O-NpSRII}}$ (NpSRII)). Taking a ratio of this factor to the thermal grating signal of the calorimetric reference sample for the sake of normalization, one may find the following relation from Eqs. 4 and 6;

$$\frac{\delta n_{\text{O-NpSRII}}(\text{pSRII} - \Delta\text{pHtrII}) - \delta n_{\text{O-NpSRII}}(\text{pSRII})}{\delta n_{\text{th}}^{0}(\textit{reference})} = V\left(\frac{dT}{dV}\right)\frac{\rho C_{\text{P}}}{h\nu W}\Delta\Delta V_{\text{O-NpSRII}}. \quad (10)$$

Using this equation and the determined $\{\delta n_6(\text{NpSRII})$-ΔNpHtrII$\delta n_6$ − (NpSRII)$\}/\delta n_{\text{th}}^{0}$(reference) = 0.9, we obtained $\Delta\Delta V_{\text{O-NpSRII}}$ to be −12 ± 3 cm^3/mol; i.e., ΔNpHtrII induces the additional volume contraction of 12 cm^3/mol for the O→ NpSRII transition. Interestingly, $\{\delta n_5$(NpSRII)-ΔNpHtrII)− δn_5 (NpSRII$\}/\delta n_{\text{th}}^{0}$(reference) for M″ → O has an opposite sign with a similar amplitude to the δn_6 process (−0.7). This fact suggests that the volume expansion of ~+12 cm^3/mol is associated with the M″ → O transition by the presence of ΔNpHtrII.

As stated above, the volume change for each species cannot be estimated because of the presence of the population grating contribution. However, we can estimate the lowest values for the volume changes as follows. According to the well-established Lorenz-Lorentz relationship, when the absorption spectrum of intermediate species shifts to blue from that of the original species, δn_{pop} is expected to be negative in general. Indeed, this is true for many chemical reaction systems (Terazima and Hirota, 1993; Okamoto et al., 1995; Terazima, 2000). Applying this general rule to the O → NpSRII transition, we expect that the population grating for this transition should be negative. The negative population grating by creation of the product means that the preexponential factor corresponding to this process should be positive. However, the observed sign of δn_6 is negative as listed in Table 1. This negative sign of δn_6 indicates that there is a significant negative contribution of the volume grating. If we assume that the population grating contribution can be neglected in the signal, ΔV associated with O → NpSRII transition for NpSRII and NpSRII-ΔNpHtrII is calculated from the $\delta n_6/\delta n_{\text{th}}$(reference) value to be −13 cm^3/mol and −25 cm^3/mol, respectively. As described above, since the population grating contribution to δn_6 is expected to be positive, this ΔV is the upper limit of the volume change (ΔV should be <-13 cm^3/mol and <-25 cm^3/mol, respectively).

DISCUSSION

First, we discuss the state of the proteins in solution from the experimentally obtained diffusion coefficients. According to the Stokes-Einstein relationship, D is given by

$$D = k_{\text{B}}T/a\eta\text{r}, \quad (11)$$

where k_{B}, T, η, and r are Boltzmann constant, temperature, viscosity, and radius of the molecule, respectively. D_{pSR} and $D_{\text{pSR-H}}$ are determined to be 3.4 ± 0.3 × 10^{-11} m^2/s and 1.81 ± 0.2 × 10^{-11} m^2/s. If we assume that the difference comes from only the difference in the protein radius, the radius of NpSRII-ΔNpHtrII should be 1.9 times larger than that of NpSRII. If we assume that the diffusing species is spherical and the molecular volume can be calculated by the third power of the radius, the volume of NpSRII-ΔNpHtrII is 6.7 times larger than that of NpSRII. Considering the molecular mass of ΔNpHtrII (18 kDa) compared with that of NpSRII (25 kDa), the molecular size of NpSRII-ΔNpHtrII cannot be so much larger than that of NpSRII to explain the difference in D. Based on these facts, we consider that the NpSRII-ΔNpHtrII exists in the dimeric form in the sample solution. Although the volume ratio of (NpSRII-ΔNpHtrII)$_2$/NpSRII (3.4) is still smaller than 6.7 predicted from the ratio of D, the difference may be explained by the experimental error and also the effect of surfactant. If we use the lowest value of D for NpSRII and largest value for NpSRII-ΔNpHtrII within the errors, the volume ratio becomes ~3.5, which is close to the expected value (3.6). Furthermore, since the number of the surfactant molecule is expected to be much larger for the larger proteins, D of (NpSRII-ΔNpHtrII)$_2$ could be smaller than that expected only from the protein volume. Previously, SRI-HtrI complex has been shown to exist in a dimeric form and to interact physically with SRI both under the light and dark conditions (Zhang and Spudich, 1998). The x-ray crystallographic data of NpSRII-ΔNpHtrII also show the dimeric form in crystal (Gordelly et al., 2002). The above finding of D is consistent with these reported data.

It is important to note that the rate constants from the TG signal are very similar to those from the TA signal. There is no additional component in the TG signal except the thermal grating contribution. This feature is quite different from other biological proteins. For example, spectrally silent dynamics,

which do not appear in the TA method, are observed in the TG signal for the photoreaction of octopus rhodopsin (Nishioku et al., 2001). The dynamics were attributed to the movement of the protein conformation distant from the chromophore, because the TA signal is sensitive to only the structural changes, which is close to the chromophore. Similarly, spectrally silent dynamics have been observed in the photodissociation reaction of carboxymyoglobin (Sakakura et al., 2001, 2002) and photoreaction of photoactive yellow protein (PYP) (Takeshita et al., 2002). The absence of the spectrally silent dynamics in this NpSRII reaction implies that the conformational change of the protein is effectively coupled with the conformational change around the chromophore, and every dynamics can be monitored by the change in the optical transition in visible region. (The slight differences in the rate constants between the TG and TA methods may be caused by possible contaminations of the spectrally silent dynamics in the TG signal.)

For NpSRII, the L intermediate possesses relatively high energy. Considering that the chromophore is completely isomerized, the instability must reside in the protein part. The energy stored in the protein moiety is then dissipated in L $\rightarrow$ M conversion. On the other hand, the conformation in L for NpSRII-ΔNpHtrII is relatively stabilized in view of smaller enthalpy in L in the fusion protein as compared to NpSRII (Fig. 5). This indicates the influence of the transducer on the structure of the photoreceptor exists as early as in L intermediate. Previously it was reported that the hydrogen bonding between Tyr-199 and Thr-204 of NpSRII is strengthened (Sudo et al., 2003) and that the peptide backbone of NpSRII is altered (Furutani et al., 2003) upon K formation, when it is in complex with ΔNpHtrII. It is tempting to speculate that the stabilization effect of the transducer on L observed in our experiment reflects this hydrogen-bonding interaction and the protein conformation change. The energy difference between NpSRII and NpSRII-ΔNpHtrII decreases on the M formation.

Since there is energetic influence of the transducer on the L conformation, this step may well be the signal transduction step from the photoreceptor to the transducer. However, because no volume change was found in the transducer in this step (see Volume Change), we do not consider that L intermediate is a signaling state.

Significant conformational changes detected as volume expansion and contraction were found in M″ $\rightarrow$ O and in O $\rightarrow$ NpSRII processes, respectively, for both NpSRII and NpSRII-ΔNpHtrII. It is particularly noteworthy that the molecular volume changes found in the last two steps of the photocycles were larger for NpSRII-ΔNpHtrII than that for NpSRII, suggesting that the transducer also undergoes conformational changes.

The interpretation of the volume change is as follows. During the reaction processes in the photocycle, the constitutive volume, which is the sum of the van der Waals volumes of all of the constitutive atoms, should be conserved. We think that the volume change during this photocycle can be explained in terms of the solvent exclusion volume, which is a volume on the surface of the molecule, where no entry by solvent molecules is allowed. If two spherical molecules contact to each other, the partial molar volume should decreases due to the loss of solvent exclusion volume around the molecule. The observed additional volume expansion during the M″ $\rightarrow$ O process by ΔNpHtrII suggests that the number of atomic contact decreases at this stage.

It was reported previously that the F-helix (seventh helix) of NpSRII tilts outward in the M state (Wegener et al., 2000; Bergo et al., 2003), accompanied by the clockwise rotation of the TM2 helix in ΔNpHtrII viewed form the cytoplasmic side. Such a movement of the helices results in disruption of the ionic- and the hydrogen-bonding interaction and loosening of the tight binding between the two protein molecules. The volume expansion in the M″ $\rightarrow$ O process observed in our experiment might, therefore, be explained by the weakened interaction, because this could result in decrease of number of atomic contacts. Alternatively, loosening of the folded structure, which also decreases number of atomic contact, could cause volume expansion. In this case, the volume increase in the M″ $\rightarrow$ O process might represent the unfolding of a tertiary structure of an as yet unresolved cytoplasmic domain or the unwinding of the coiled coil in the cytoplasmic domain of ΔNpHtrII. In any case, the volume increase observed in the fusion protein in the M″ $\rightarrow$ O process, which is larger than the expansion in the receptor alone, presents a strong evidence that the signaling state of NpSRII is the last intermediate O and that conformational changes are coupled between the photoreceptor and the transducer in the O state. This evidence is in keeping with the general concept that the sensory photoreceptors photocycle intermediates with longer lifetimes to attain efficient signal transduction to the effector molecules, in contrast to the analogous photoreceptors functioning as electrogenic ion pumps such as bacteriorhodopsin and halorhodopsin.

CONCLUSION

Dynamics of the protein conformational changes of pharaonis sensory rhodopsin II (NpSRII) and the protein-protein interaction of NpSRII-transducer protein (ΔNpHtrII) complex are investigated at room temperature by the laser flash photolysis and the transient grating methods. We found that the diffusion coefficient of NpSRII-ΔNpHtrII is significantly smaller than that of NpSRII. This smaller D indicates that the NpSRII-ΔNpHtrII complex exists in a dimeric form in the DM solution. Rate constants of the reaction processes determined from the transient absorption and grating methods agree quite well. The absorption spectrum of NpSRII-ΔNpHtrII is almost identical to that of NpSRII. The effects of ΔNpHtrII on NpSRII were less significant in the photocycle kinetics but were large in the volume change and in the molecular energy. The enthalpy of the second intermediate

(L) of NpSRII-ΔNpHtrII is more stabilized compared with that of NpSRII. This stabilization indicates the influence of the transducer to the NpSRII structure in the early intermediate species by the complex formation. Relatively large molecular volume expansion and contraction were observed in the last two steps for NpSRII. Additional volume expansion and contraction were induced by the presence of ΔNpHtrII for the last two steps. This volume change is interpreted in terms of a decrease in the number of atomic contact as a possible result of loosening of the interaction between the two molecules or loosening of tertiary structure in the M″ → O process. The volume change is returned (contraction) to the original state in the last step, O → NpSRII. The conformational change induced by the transducer protein suggests that the O state is the signal transduction process of the NpSRII-ΔNpHtrII complex. We believe that this time-resolved measurement of the volume change during reactions will be a powerful tool to study the protein-protein interaction in solution in real time.

This work is supported by the Grant-in-Aid (13853002 and 13853002) from the Ministry of Education, Science, Sports, and Culture in Japan.

REFERENCES

Bergo, V., E. N. Spudich, J. L. Spudich, and K. J. Rothschild. 2003. Conformational changes detected in a sensory rhodopsin II-transducer complex. *J. Biol. Chem.* 278:36556–36562.

Bogomolni, R. A., and J. L. Spudich. 1982. Identification of a third rhodopsin-like pigment in phototactic *Halobacterium halobium. Proc. Natl. Acad. Sci. USA*. 79:6250–6254.

Bogomolni, R. A., W. Stoekenius, I. Szundi, E. Perozo, K. D. Olson, and J. L. Spudich. 1994. Removal of transducer HtrI allows electrogenic proton translocation by sensory rhodopsin I. *Proc. Natl. Acad. Sci. USA*. 91:10188–10192.

Braslavsky, S. E., and G. E. Heibel. 1992. Time-resolved photothermal and photoacoustic methods applied to photoinduced processes in solution. *Chem. Rev.* 92:1381–1410.

Chen, X., and J. L. Spudich. 2002. Demonstration of 2:2 stoichiometry in the functional SRI-HtrI signaling complex in *Halobacterium* membranes by gene fusion analysis. *Biochemistry*. 41:3891–3896.

Chizhov, I., G. Schmies, R. Seidel, J. R. Sydor, B. Lüttenberg, and E. Engelhard. 1998. The photophobic receptor from Natronobacterium pharaonis: temperature and pH dependencies of the photocycle of sensory rhodopsin II. *Biophys. J.* 75:999–1009.

Falke, J. J., and G. L. Hazelbauer. 2001. Transmembrane signaling in bacterial chemoreceptors. *Trends Biochem. Sci.* 26:257–265.

Furutani, Y., Y. Sudo, N. Kamo, and H. Kandori. 2003. FTIR spectroscopy of the complex between *pharaonis* phoborhodopsin and its transducer protein. *Biochemistry*. 42:4837–4842.

Gordelly, V. I., J. Labahn, R. Moukhametzianov, R. Efremov, J. Granzin, R. Schlesinger, G. Büldt, T. Savopol, A. J. Scheldlg, J. P. Klare, and M. Engelhard. 2002. Molecular basis of transmembrane signalling by sensory rhodopsin II-transducer complex. *Nature*. 419:484–487.

Hara, T., N. Hirota, and M. Terazima. 1996. New application of the transient grating method to a photochemical reaction: the enthalpy, reaction volume change, and partial molar volume measurements. *J. Phys. Chem.* 100:10194–10200.

Hirayama, J., Y. Imamoto, Y. Shichida, N. Kamo, H. Tomioka, and T. Yoshizawa. 1992. Photocycle of phoborhodopsin from haloalkaliphilic bacterium (Natronobacterium pharaonis) studied by low-temperature spectrophotometry. *Biochemistry*. 31:2093–2098.

Hoppler-Mreyen, S., J. P. Klare, A. A. Wegener, R. Seidel, C. Herrmann, G. Schmies, G. Nagel, E. Bamberg, and M. Egelhard. 2003. Probing the sensory rhodopsin II binding domain of its cognate transducer by calorimetry and electrophysiology. *J. Mol. Biol.* 330:1203–1213.

Imamoto, Y., Y. Shichida, T. Yoshizawa, H. Tomioka, T. Takahashi, K. Fujikawa, N. Kamo, and Y. Kobatake. 1991. Photoreaction cycle of phoborhodopsin studied by low-temperature spectroscopy. *Biochemistry*. 30:7416–7424.

Jung, K.-H., E. N. Spudich, V. D. Trivedi, and J. L. Spudich. 2001. An archaeal photosignal-transducing module mediates phototaxis in Escherichia coli. *J. Bacteriol.* 183:6365–6371.

Krebs, M. P., E. N. Spudich, H. G. Khorana, and J. L. Spudich. 1993. Synthesis of a gene for sensory rhodopsin I and its functional expression in *Halobacterium halobium. Proc. Natl. Acad. Sci. USA*. 90:3486–3490.

Krebs, M. P., E. N. Spudich, and J. L. Spudich. 1995. Rapid high-yield purification and liposome reconstitution of polyhistidine-tagged sensory rhodopsin I. *Protein Expr. Purif.* 6:780–788.

Kunji, E. R., E. N. Spudich, R. Grisshammer, R. Henderson, and J. L. Spudich. 2001. Electron crystallographic analysis of two-dimensional crystals of sensory rhodopsin II: a 6.9 Å projection structure. *J. Mol. Biol.* 308:279–293.

Losi, A., and S. E. Braslavsky. 2003. The time-resolved thermodynamics of the chromophore-protein interactions in biological photosensors as derived from photothermal measurements. *Phys. Chem. Chem. Phys.* 5:2739–2750.

Losi, A., A. A. Wegener, M. Engelhard, and S. E. Braslavsky. 2001a. Enthalpy-entropy compensation in a photocycle: the K-to-L transition in sensory rhodopsin II from *Natronobacterium pharaonis*. *J. Am. Chem. Soc.* 123:1766–1767.

Losi, A., A. A. Wegener, M. Engelhard, and S. E. Braslavsky. 2001b. Thermodynamics of the early steps in the photocycle of *Natronobacterium pharaonis* halorhodopsin. Influence of medium and of anion substitution. *Photochem. Photobiol.* 74:495–503.

Losi, A., A. A. Wegener, M. Engelhard, W. Gärtner, and S. E. Braslavsky. 1999. Time-resolved absorption and photothermal measurements with recombinant sensory rhodopsin II from *Natronobacterium pharaonis*. *Biophys. J.* 77:3277–3286.

Luecke, H., B. Schobert, J. K. Lanyi, E. N. Spudich, and J. L. Spudich. 2001. Crystal structure of sensory rhodopsin ii at 2.4 angstroms: insights into color tuning and transducer interaction. *Science*. 293:1499–1503.

Lüttenberg, B., E. K. Wolff, and M. Engelhard. 1998. Heterologous coexpression of the blue light receptor psRII and its transducer pHtrII from *Natronobacterium pharaonis* in the *Halobacterium salinarium* strain Pho81/w restores negative phototaxis. *J. Am. Chem. Soc.* 123: 1766–1767.

Mukohata, Y. 1994. Comparative studies on ion pumps of the bacterial rhodopsin family. *Biophys. Chem.* 50:191–201.

Nishioku, Y., M. Nakagawa, M. Tsuda, and M. Terazima. 2001. A spectrally silent transformation in the photolysis of octopus rhodopsin: a protein conformational change without any accompanying change of the chromophore's absorption. *Biophys. J.* 80:2922–2927.

Nishioku, Y., M. Nakagawa, M. Tsuda, and M. Terazima. 2002. Energetics and volume changes of the intermediates in the photolysis of octopus rhodopsin at a physiological temperature. *Biophys. J.* 83:1136–1146.

Okamoto, K., M. Terazima, and N. Hirota. 1995. Temperature dependence of diffusion processes of radical intermediates probed by the transient grating method. *J. Chem. Phys.* 103:10445–10452.

Parkinson, J. S. 2003. Bacterial chemotaxis: a new player in response regulator dephosphorylation. *J. Bacteriol.* 185:1492–1494.

Royant, A., P. Nollert, K. Edman, R. Neutze, E. M. Landau, E. Pebay-Peyroula, and J. Navarro. 2001. X-ray structure of sensory rhodopsin II at 2.1-A resolution. *Proc. Natl. Acad. Sci. USA*. 98:10131–10137.

Sakakura, M., I. Morishima, and M. Terazima. 2002. Structural dynamics of distal histidine replaced mutants of myoglobin accompanied with the photodissociation reaction of the ligand. *Biochemistry.* 41:4837–4846.

Sakakura, M., S. Yamaguchi, N. Hirota, and M. Terazima. 2001. Dynamics of structure and energy of horse carboxymyoglobin after photodissociation. *J. Am. Chem. Soc.* 123:4286–4294.

Sasaki, J., and J. L. Spudich. 1998. The transducer protein HtrII modulates the lifetimes of sensory rhodopsin II photointermediates. *Biophys. J.* 75:2435–2440.

Schmies, G., B. Luttenberg, I. Chizhov, M. Engelhard, A. Becker, and E. Bamberg. 2000. Sensory rhodopsin II from the haloalkaliphilic natronobacterium pharaonis: light-activated proton transfer reactions. *Biophys. J.* 78:967–976.

Seidel, R., B. Scharf, M. Gautel, K. Kleine, D. Oesterhelt, and M. Engelhard. 1995. The primary structure of sensory rhodopsin II: a member of an additional retinal protein subgroup is coexpressed with its transducer, the halobacterial transducer of rhodopsin II. *Proc. Natl. Acad. Sci. USA.* 92:3036–3040.

Simono, K., M. Iwamoto, M. Sumi, and N. Kamo. 1997. Functional expression of pharaonis phoborhodopsin in Escherichia coli. *FEBS Lett.* 420:54–56.

Spudich, J. L., and R. A. Bogomolni. 1984. Mechanism of colour discrimination by a bacterial sensory rhodopsin. *Nature.* 312:509–513.

Spudich, E. N., and J. L. Spudich. 1993. The photochemical reactions of sensory rhodopsin I are altered by its transducer. *J. Biol. Chem.* 268: 16095–16097.

Spudich, E. N., S. A. Sundberg, D. Manor, and J. L. Spudich. 1986. Properties of a second sensory receptor protein in Halobacterium halobium. *Proteins.* 1:239–246.

Spudich, J. L., C. S. Yang, K. H. Jung, and E. N. Spudich. 2000. Retinylidene proteins: structures and functions from archaea to humans. *Annu. Rev. Cell Dev. Biol.* 16:365–392.

Stock, J. B., M. N. Levit, and P. M. Wolanin. 2002. Information processing in bacterial chemotaxis. *Sci. STKE.* 2002:PE25.

Sudo, Y., Y. Furutani, K. Shimono, N. Kamo, and H. Kandori. 2003. Hydrogen bonding alteration of Thr-204 in the complex between *pharaonis* phoborhodopsin and its transducer protein. *Biochemistry.* 42:14166–14172.

Sudo, Y., M. Iwamoto, K. Shimono, and N. Kamo. 2001. Pharaonis phoborhodopsin binds to its cognate truncated transducer even in the presence of a detergent with a 1:1 stoichiometry. *Photochem. Photobiol.* 74:489–494.

Sudo, Y., M. Iwamoto, K. Shimono, and N. Kamo. 2002. Association between a photo-intermediate of a M-lacking mutant D75N of pharaonis phoborhodopsin and its cognate transducer. *J. Photochem. Photobiol. B.* 67:171–176.

Takahashi, T., H. Tomioka, N. Kamo, and Y. Kobatake. 1985. A photosystem other than PS370 also mediates negative phototaxis of *Halobacterium halobium*. *FEMS Microbiol. Lett.* 28:161–164.

Takeshita, K., Y. Imamoto, M. Kataoka, K. Mihara, F. Tokunaga, and M. Terazima. 2002. Structural change of site-directed mutants of PYP: new dynamics during pR state. *Biophys. J.* 83:1567–1577.

Terazima, M. 1998. Photothermal studies of photophysical and photochemical processes by the transient grating method. *Adv. Photochem.* 24:255–338.

Terazima, M. 2000. Translational diffusion of organic radicals in solution. *Acc. Chem. Res.* 33:687–694.

Terazima, M., and N. Hirota. 1993. Translational diffusion of a transient radical studied by the transient grating method, pyrazinyl radical in 2-propanol. *J. Chem. Phys.* 98:6257–6262.

Wegener, A.-A., I. Chizhov, M. Engelhard, and H.-J. Steinhoff. 2000. Time-resolved detection of transient movement of helix F in spin-labelled pharaonis sensory rhodopsin II. *J. Mol. Biol.* 301:881–891.

Yao, V. J., and J. L. Spudich. 1992. Primary structure of an archaebacterial transducer, a methyl-accepting protein associated with sensory rhodopsin I. *Proc. Natl. Acad. Sci. USA.* 89:11915–11919.

Zhang, W., A. Brooun, M. M. Mueller, and M. Alam. 1996. The primary structures of the archaeon *Halobacterium salinarium* blue light receptor sensory rhodopsin II and its transducer, a methyl-accepting protein. *Proc. Natl. Acad. Sci. USA.* 93:8230–8235.

Zhang, D., and D. Mauzerall. 1996. Volume and enthalpy changes in the early steps of bacteriorhodopsin photocycle studied by time-resolved photoacoustics. *Biophys. J.* 71:381–388.

Zhang, X.-N., and J. L Spudich. 1998. HtrI is a dimer whose interface is sensitive to receptor photoactivation and His-166 replacements in sensory rhodopsin I. *J. Biol. Chem.* 273:19722–19728.

Zhang, X.-N., J. Zhu, and J. L Spudich. 1999. The specificity of interaction of archaeal transducers with their cognate sensory rhodopsins is determined by transmembrane helices. *Proc. Natl. Acad. USA.* 96:857–862.